Polymer Journal

Acceleration Mechanism in Critical Nucleation of Polymers by Epitaxy of Nucleating Agent

By Tsuyoshi URUSHIHARA,[1,*] Kiyoka OKADA,[2] Kaori WATANABE,[2] Akihiko TODA,[2] Naoshi KAWAMOTO,[1] and Masamichi HIKOSAKA[2]

Effect of epitaxy of nucleating agent (NA) on nucleation of polymers was investigated based on kinetic study. Nucleation rate (I) of polymers is given by $I = I_0 \exp(-\Delta G^*/kT_c)$ (1), where I_0 is prefactor, ΔG^* is free energy for forming critical nucleus, k is Boltzmann constant and T_c is crystallization temperature. We reported in the previous paper that decreasing the size of NA is important for increasing I_0, $i.e.$, I. In this study we focus on ΔG^* dependence of I. In the case of heterogeneous nucleation, ΔG^* is a function of interfacial free energy between NA and nucleus ($\Delta \sigma$). $\Delta \sigma/\sigma$ varies between 0 and 1 where σ is lateral surface free energy of nucleus. $\Delta \sigma/\sigma$ of isotactic polypropylene (iPP) mixed with three NAs were between 0.13 and 0.23, which were evaluated by the fit of eq 1 to the experimental data of I. I increased by 38 orders of magnitude for $\Delta T = 30\,\mathrm{K}$ with decreasing $\Delta \sigma/\sigma$ from 1 to 0. In the case of NA, I increased by 60 times for $\Delta T = 30\,\mathrm{K}$ with decreasing $\Delta \sigma/\sigma$ from 0.23 to 0.13. I significantly depends on $\Delta \sigma$. Therefore we concluded that $\Delta G^*(\Delta \sigma)$ is essentially important for acceleration of nucleation.
KEY WORDS: Nucleating Agent / Epitaxy / Nucleation / Polypropylene /

In our previous study, acceleration mechanism of heterogeneous nucleation by nucleating agent (NA) was investigated based on kinetic study.[1,2] In the classical nucleation theory (CNT) nucleation rate I is generally expressed as a product of two factors, prefactor I_0 and probability of forming a critical nucleus,[3,4]

$$I = I_0 \exp\left(-\frac{\Delta G^*}{kT_c}\right) \quad (1)$$

where ΔG^* is free energy for forming critical nucleus, k is Boltzmann constant and T_c is crystallization temperature.

In our previous studies,[1,2] acceleration mechanism of the first factor of I_0 by NA was studied by assuming epitaxy between NA and polymer crystals. The acceleration mechanism by ΔG^* in heterogeneous nucleation has not been studied based on kinetic study. Purpose of this study is to clarify the important role of ΔG^* in acceleration mechanism of heterogeneous nucleation.

I_0 was predicted in our previous study by

$$I_0 \propto C_{NA} a_{NA}^{-1}, \quad (2)$$

where C_{NA} is concentration of NA in the mixture of NA and polymer and a_{NA} is the largest lateral size of a NA crystal.[1] Eq 2 was confirmed experimentally in our previous study.[1,2] It is concluded that I_0 is accelerated by significant epitaxy between NA and iPP crystals.

Role of $\Delta G^*(\Delta \sigma)$ in Acceleration of Heterogeneous Nucleation

In this study, we will focus on the second factor of eq 1, ΔG^*.[3,4] When we assume rectangular parallelepiped nucleus

on the basis of CNT,[5] ΔG of heterogeneous nucleation is given by

$$\Delta G = -lmn\Delta g + 2lm\sigma + 2mn\sigma_e + ln\Delta \sigma \quad (3)$$

where l, m and n are the length of each edge of a nucleus, Δg is the bulk free energy of fusion, σ and σ_e are lateral and end surface free energy, respectively, and $\Delta \sigma$ is defined by

$$\Delta \sigma \equiv \sigma + \sigma_{0s} - \sigma_s, \quad (4)$$

where σ_{0s} and σ_s are the interfacial energy between nucleus and heterogeneity and the surface free energy of heterogeneity, respectively. In this study, l, m, n are counted by repeating unit, and Δg, σ, σ_e, σ_{0s}, σ_s, and $\Delta \sigma$ are defined per repeating unit. Eq 3 represents hypersurface, and the position of extremum designates ΔG^*. The positions of l, m and n with respect to ΔG^* are defined by l^*, m^*, n^*. When we set m the length along a direction normal to epitaxial plane of NA, m^* is the critical value in relation to the dimension of critical nucleus, which is given by

$$m^* = \frac{2\Delta \sigma}{\Delta g}. \quad (5)$$

When $m^* > 1$, $i.e.$, $\Delta g < 2\Delta \sigma$, three dimensional (3D) nucleation takes place. In the case of $m^* < 1$, $i.e.$, $\Delta g > 2\Delta \sigma$, two dimensional (2D) nucleation occurs. ΔG^*'s of 3D and 2D nucleation (ΔG^*_{3D} and ΔG^*_{2D}, respectively) are expressed by

$$\Delta G^*_{3D}(\Delta \sigma) = \frac{16\sigma\sigma_e\Delta \sigma}{\Delta g^2} \quad \text{for} \quad m^* > 1, \ \Delta g < 2\Delta \sigma \quad (6)$$

and

[1]ADEKA Corporation, 5-2-13, Shirahata, Minami-ku, Saitama 336-0022, Japan
[2]Graduate School of Integrated Arts and Sciences, Hiroshima University, 1-7-1 Kagamiyama, Higashihiroshima 739-8521, Japan
*To whom correspondence should be addressed (Tel: +81-48-838-2244, Fax: +81-48-838-2250, E-mail: urushi@adeka.co.jp).

$$\Delta G_{2D}^*(\Delta\sigma) = \frac{4\sigma\sigma_e}{\Delta g - \Delta\sigma} \quad \text{for} \quad m \leq 1, \ \Delta g \geq 2\Delta\sigma, \quad (7)$$

respectively. From eq 5 and thermodynamic relation given by

$$\Delta g = \frac{\Delta h \Delta T}{T_m^0} \quad (8)$$

where Δh is enthalpy of fusion, ΔT is degree of supercooling and T_{m}^0 is equilibrium melting temperature,[5] the supercooling temperature of conversion from 3D to 2D nucleation $\Delta T_{2D/3D}$ is given by

$$\Delta T_{2D/3D} = \frac{2\Delta\sigma T_{\mathrm{m}}^0}{\Delta h}. \quad (9)$$

Importance of $\Delta\sigma$ for Study of NA

Even CNT showed that ΔG^* depends on $\Delta\sigma$ as described in eqs 6 and 7, kinetic studies of nucleation based on CNT in the past have not paid much attention to $\Delta\sigma$ and $\Delta T_{2D/3D}$. As some heterogeneity must inherently be included without trying to remove it carefully, we have to take heterogeneous effect, *i.e.*, $\Delta\sigma$, into account. NA has much smaller $\Delta\sigma$ than a mere heterogeneity so that $\Delta T_{2D/3D}$ of a polymer with NA is smaller than that without NA. Therefore we have to choose the appropriate formulation of 3D or 2D nucleation as to $\Delta\sigma$ and $\Delta T_{2D/3D}$. But the evaluation method of $\Delta\sigma$ has not been established yet. In this study we will show how to determine $\Delta\sigma$.

When we assume that σ_{0s} changes from 0 to σ, $\Delta\sigma$ changes from 0 to σ, *i.e.*,

$$\Delta\sigma = 0 \sim \sigma \quad \text{or} \quad \Delta\sigma/\sigma = 0 \sim 1, \quad \text{for} \quad \sigma_{0s} = 0 \sim \sigma. \quad (10)$$

In this study we use $\Delta\sigma/\sigma$. When $\Delta\sigma/\sigma = 0$, the nucleus becomes an ideal NA. This corresponds to the secondary nucleation. When $\Delta\sigma/\sigma = 1$, the epitaxy between heterogeneity and nucleus is negligible. ΔG^* decreases with decrease of $\Delta\sigma/\sigma$. This results in acceleration of I. In the case of heterogeneity with small $\Delta\sigma/\sigma$, *i.e.*, $\Delta\sigma/\sigma \ll 1$, it is named NA. As $\Delta\sigma/\sigma$ of NA is not commonly given, we will name the heterogeneity as NA when

$$\Delta\sigma/\sigma < 0.3 \quad (11)$$

is satisfied in this study.

Epitaxy of NAs

Epitaxy comes from an interaction between two contact planes of the crystals. Thus efficiency of epitaxy should be controlled by two dimensional lattice matches in the contact planes. Degree of misfit (δ) for an azimuthal orientation in the contact planes is defined by

$$\delta = \frac{d - d_s}{d} \times 100 \ (\%), \quad (12)$$

where d and d_s are lengths of the approximate least common multiple of lattice constants of an overgrowth layer and substrate, respectively.[6] Epitaxy should take place when absolute value of δ is small.
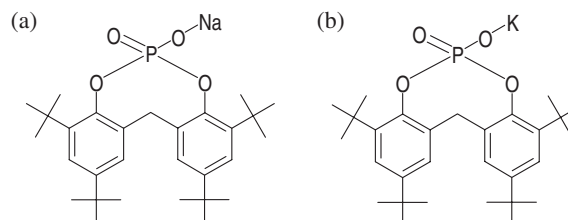

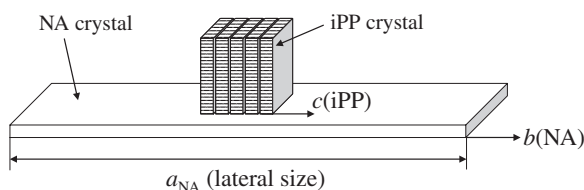**Figure 1.** Chemical structure of (a) NA-11 and (b) NA-11K.

Figure 2. Epitaxial relationship between NA-11 and iPP crystals.

In this study, iPP was used as a typical polymer. As a typical high-performance NA for iPP, sodium 2,2′-methylene-bis-(4,6-di-*t*-butylphenylene)phosphate (ADEKA Corp., NA-11) was used. The structure of NA-11 is shown in Figure 1a. Kawaguchi *et al.* reported that the epitaxial relationship between NA-11 and iPP crystals,[7]

$$b(\text{NA-11}) \ // \ c(\text{iPP}) \quad (13)$$

where $b(\text{NA-11})$ and $c(\text{iPP})$ are crystal lattice constants of b of NA-11 and c of iPP, respectively. This is schematically shown in Figure 2. As the other azimuthal orientation in the contact planes is not specified, we will only evaluate lattice matching for one azimuthal orientation in eq 13. In this study, substrate, *i.e.*, NA, will be changed for a polymer, *i.e.*, iPP. Eq 12 can be rewritten as

$$\delta' = \frac{d(\text{iPP}) - d(\text{NA})}{d(\text{iPP})} \times 100 \ (\%) \quad (14)$$

where δ' is degree of misfit between NA and iPP crystals, $d(\text{iPP})$ and $d(\text{NA})$ are the lattice constants for an azimuthal orientation in the contact planes. As $b(\text{NA-11})$ and $c(\text{iPP})$ are

$$b(\text{NA-11}) = 0.608 \ (\text{nm}) \quad \text{and} \quad c(\text{iPP}) = 0.65 \ (\text{nm}), \quad (15)$$

respectively,[5,8] δ' given by eq 14 becomes

$$\delta' = +6.5 \ (\%). \quad (16)$$

Crystal lattice match between NA-11 and iPP is not good enough. In order to decrease δ', the sodium Na atom in NA-11 was substituted by a larger atom of potassium K, *i.e.*, potassium 2,2′-methylene-bis-(4,6-di-*t*-butylphenylene) phosphate (Figure 1b) was synthesized. As a typical conventional NA, sodium benzoate was used. The unit cell structure of sodium benzoate has not been reported. As sodium benzoate shows lower performance, $\Delta\sigma$ of sodium benzoate should be larger than that of NA-11.

Purpose

The first purpose of this study is to clarify the free energy of forming critical nucleus $\Delta G^*(\Delta\sigma)$ dependence of the nucleation rate I based on the nucleation theory, where $\Delta\sigma$ is a kinetic parameter reflected in efficiency of epitaxy. Clarification of the effect of $\Delta G^*(\Delta\sigma)$ on I is important for understanding a role of epitaxy of NA in heterogeneous nucleation. The second purpose of this study is to clarify the effect of $\Delta\sigma$ on the geometrical manner of nucleation, *i.e.*, three or two dimensional (3D or 2D) ones, and to establish the evaluation method of $\Delta\sigma$. Understanding of supercooling temperature of 3D-2D conversion $\Delta T_{2D/3D}$ is the need for determination of $\Delta\sigma$. And the evaluation method of $\Delta\sigma$ should be useful for quantitative analysis of the ability of NA.

THEORETICAL

Conversion of $I(\Delta\sigma)$ at $\Delta T_{2D/3D}$

Formulation of $I(\Delta\sigma)$ as a function of ΔT is useful for kinetic study. Insertion of eqs 6 or 7 into eq 1 gives I of 3D or 2D nuclei (I_{3D} or I_{2D}, respectively). Here I_{3D} and I_{2D} are divided by I_0 to eliminate the effect of I_0 on I. I_{3D}/I_0 and I_{2D}/I_0 are given by

$$\frac{I_{3D}(\Delta\sigma)}{I_0} = \exp\left(-\frac{\Delta G^*_{3D}}{kT_c}\right) = \exp\left(-\frac{C}{T_c\Delta T^2}\right)$$
$$\text{for} \quad \Delta g < 2\Delta\sigma \quad (17)$$

where

$$C(\Delta\sigma) = \frac{16\sigma\sigma_e\Delta\sigma T_m^{0\,2}}{k\Delta h^2} \quad (18)$$

and

$$\frac{I_{2D}(\Delta\sigma)}{I_0} = \exp\left(-\frac{\Delta G^*_{2D}}{kT_c}\right) = \exp\left\{-\frac{\alpha(\Delta\sigma)B}{T_c\Delta T}\right\}$$
$$\text{for} \quad \Delta g \geq 2\Delta\sigma \quad (19)$$

where

$$\alpha(\Delta\sigma) \equiv \frac{\Delta g}{\Delta g - \Delta\sigma} = \frac{\Delta h\Delta T}{\Delta h\Delta T - \Delta\sigma T_m^0}$$
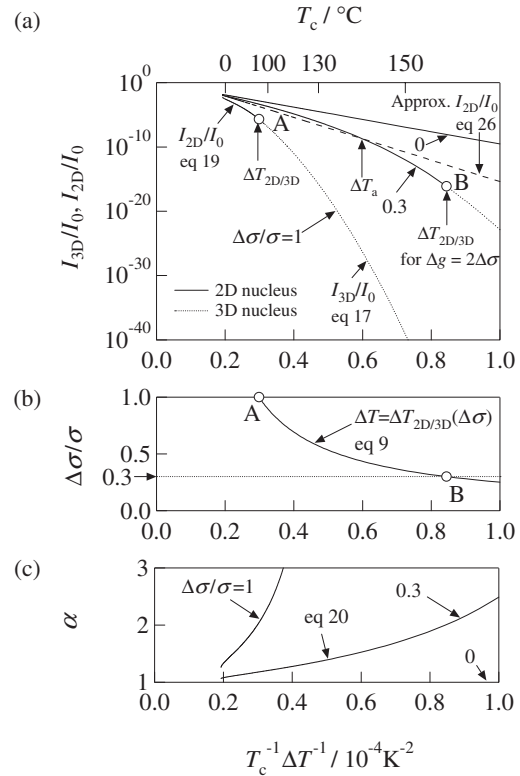$$\text{and} \quad B = \frac{4\sigma\sigma_e T_m^0}{k\Delta h}, \quad (20)$$

respectively.

When $\Delta\sigma/\sigma = 0$, α in eq 20 becomes 1. Therefore we can rewrite eq 19 as

$$\frac{I_{2D}(\Delta\sigma = 0)}{I_0} = \exp\left(-\frac{\Delta G^*_{2D}(\Delta\sigma = 0)}{kT_c}\right)$$
$$= \exp\left\{-\frac{B}{T_c\Delta T}\right\}. \quad (21)$$

From the eqs 21 and A·3,

$$\frac{I_{2D}(\Delta\sigma = 0)}{I_0} = \left(\frac{V}{V_0}\right)^\gamma \quad (22)$$

where V and V_0 are the lateral growth rate and a prefactor, respectively, $\gamma = 1$ or 3 corresponds to single or multi nucleation, respectively.

Figure 3. (a) Theoretical curves of I_{2D}/I_0 and I_{3D}/I_0 of iPP against $T_c^{-1}\Delta T^{-1}$ as a parameter of $\Delta\sigma/\sigma$. Dimension of the shape of primary nucleus changes at $\Delta T_{2D/3D}$ where $\Delta g = 2\Delta\sigma$. Upper axis indicates T_c. Solid line and curves show I_{2D}/I_0 and dotted curves show I_{3D}/I_0. I decreases with increase of $\Delta\sigma/\sigma$ for a constant T_c. A and B corresponds to those in (b). Broken line shows approximated I_{2D}/I_0 of eq 26 in the range of $\Delta T = 30$–$50\,K$. (b) Theoretical curve of $\Delta\sigma/\sigma$ against $T_c^{-1}\Delta T^{-1}$. $\Delta T_{2D/3D}$ decreases with increase of $\Delta\sigma/\sigma$. (c) Theoretical curves of α against $T_c^{-1}\Delta T^{-1}$ as a parameter of $\Delta\sigma/\sigma$. α increases with increase of $\Delta\sigma/\sigma$. α approaches to 1 with decrease of $\Delta\sigma/\sigma$.

Approximated Analysis of I_{2D} for $\alpha \cong constant$

In $\Delta G^*_{2D} = k\alpha B/\Delta T$ in eq 19, α given by eq 20 is a function of $\Delta\sigma$ and ΔT, *i.e.*,

$$\alpha = \alpha(\Delta\sigma, \Delta T). \quad (23)$$

This is the reason why I_{2D}/I_0 of eq 19 shows curvature against $T_c^{-1}\Delta T^{-1}$ in Figure 3. When $\Delta\sigma/\sigma$ is small and observed range of ΔT is limited to rather narrow range, α can be regarded to be constant as shown in Figure 3c. In this case α is approximated by a constant α_a which is given by

$$\alpha_a \equiv \alpha(\Delta\sigma, \Delta T_a) \quad (24)$$

where ΔT_a is averaged ΔT between the smallest and largest ΔT (ΔT_S and ΔT_L, respectively). ΔT_a is defined by

$$\frac{1}{\Delta T_a} = \frac{\dfrac{1}{\Delta T_S} + \dfrac{1}{\Delta T_L}}{2}. \quad (25)$$

In this case αB becomes constant. Therefore I_{2D}/I_0 against $T_c^{-1}\Delta T^{-1}$ in Figure 3 can be approximated by a straight line given by

σ/Jm^{-2}	1.15×10^{-2} [9]
σ_e/Jm^{-2}	5.5×10^{-2} [10]
$\sigma\sigma_e$/J^{2}m^{-4}	6.33×10^{-4} [9,10]
Δh/Jm^{-3}	2.09×10^{8} [11]
T_m^0/K	455.75 [12–14]

$$\frac{I_{2D}}{I_0} = \exp\left(-\frac{\alpha_a B}{T_c \Delta T}\right). \tag{26}$$

Broken line in Figure 3a is approximated I_{2D}/I_0 of eq 26 in the range of $\Delta T = 30\text{–}50\,\text{K}$. The broken line was shifted to intersect with the curve of I_{2D}/I_0 at ΔT_a by changing I_0. This approximation will be confirmed in Figure 11.

EXPERIMENTAL

Materials and Sample Preparation

Typical polymer of iPP (the number average molecular weight $M_n = 6.4 \times 10^4$, the weight average molecular weight $M_w = 3.0 \times 10^5$, the molecular weight distribution $M_w/M_n = 4.6$ and a meso pentad fraction [mmmm] = 97%) was used. Parameters of iPP crystals used in this study are shown in Table I.[9–14] T_m^0 of iPP was estimated from the relationship between M_n and tacticity.[12–14] Repeating unit of iPP was assumed that the folding direction is along (110).

Typical high-performance NA of sodium 2,2′-methylene-bis-(4,6-di-t-butylphenylene)phosphate (ADEKA Corp., NA-11) was used. To improve lattice matching between NA-11 and iPP crystals, potassium 2,2′-methylene-bis-(4,6-di-t-butylphen-ylene)phosphate (NA-11K) shown in Figure 1b was synthe-sized as follows. NA-11 of 25.4 g (0.05 mol), methanol (KOKUSAN chemical Co., Ltd.) of 250 mL and distilled water of 50 mL were mixed, and then 1N HCl aqueous solution (KOKUSAN chemical Co., Ltd.) of 60 mL (0.06 mol) was dropped onto the mixture at room temperature T_R with vigorous stirring. After finished dropping, the mixture was stirred at T_R for 1 h. The solid mass which precipitated was collected by filtration and washed three times by water of each 50 mL. Obtained crude product was solved in methanol of 600 mL, heated up to 60 °C. Distilled water of 600 mL was dropped onto the solution at 60 °C, and then the mixture was cooled to T_R. Precipitated product was filtered and dried. The yield of the product was 20.9 g (86.1%). The product of 12.2 g (0.025 mol) and methanol of 120 mL was mixed, and sub-sequently 1N KOH aqueous solution (KOKUSAN chemical Co., Ltd.) of 25.8 mL (0.0258 mol) was added onto the mixture little by little at T_R with vigorous stirring, followed by stirring at T_R for 1 h. After that, about 60 mL of the solvent was evaporated under reduced pressure at T_R. The product was filtered and washed three times by water of each 20 mL, and then dried. The yield of the product (NA-11K) was 9.1 g (69.5%). The product assignment and purity were analyzed by means of ^{1}H NMR (JEOL, Ltd., FT NMR Lambda 400), IR spectroscopy (SHIMADZU Co., FT/IR-7500) and ICP

(SHIMADZU, ICPS-7500). The purity was over 99% and sodium content was under the detective limit (<1 ppm). The obtained NA-11K crystal was grinded by a vibrating mill (CMT Co., Ltd., TI-500ET). As a conventional NA, sodium benzoate (ADEKA PALMAROLE SAS, MI.NA.08) was used. Hereafter this material will be named "Na-Bz."

Mean lateral size of NAs ($\overline{a_{NA}}$) was derived from the size distribution $f(a_{NA})$ which is measured from the SEM photo-graphs.[2] NA crystal was uniformly mixed with solution of iPP and xylene at 130 °C. The suspension was quenched to T_R, and then dried. The sample of iPP mixed with NA will be described as iPP/NA.

Instrumentals

OM and SEM. Morphology of NA crystal was observed by means of optical microscope (OM), OLYMPUS BX-51, and scanning electron microscope (SEM), Topcon SM-520.

WAXS. Wide angle X-ray scattering (WAXS) measurement was performed on the diffractometer, (Rigaku Corp., RINT-UltimaIII). All the samples were examined by CuKα radiation monochromatized by graphite crystal at T_R. Divergence slit of $1/2°$ was used. Slit width for the incidence and receiving beam were 0.73 and 0.3 mm, respectively. Scattering intensity $I_x(2\theta)$ was obtained by means of scintillation counter.

DSC. DSC measurement was conducted by means of Dia-mond DSC (PerkinElmer Inc.). Temperature was calibrated by using melting temperature of standard materials, indium and tin. The sample weighed about 2 mg was put in the aluminum pan and crimped with the aluminum rid. C_{NA} of all samples was 0.1 wt %. The sample was heated up to 230 °C at the cooling rate of 50 K/min and then held for 5 min. After that the sample was cooled to 50 °C at the rate of 10 K/min. Crystallization peak temperature (T_c) was observed. Baseline was leveled by using the software (PerkinElmer Inc., Pyris).

Crystallization of iPP

Crystallization behaviors of iPP/NA were observed by using OM, OLYMPUS BX-51, with hot stage, LINKAM LK-600PM, under nitrogen flow of 50 mL/min. Temperature of the hot stage was calibrated by using melting temperature of standard materials, indium and tin. Sample was once melted at 210 °C for 1 min, and then crystallized in the range of $T_c = 127.0\text{–}148.8\,°C$. The time t dependence of the number density $v(t)$ of iPP crystals which are larger than 2 μm in lateral size was observed. I is defined by

$$I \equiv \frac{dv(t)}{dt}. \tag{27}$$

RESULTS AND DISCUSSION

Theoretical Prediction of Significant Role of $\Delta\sigma$ in $I(\Delta T)$

It is interesting to predict how $\Delta\sigma$ affects $I(\Delta T)$ signifi-cantly when $\Delta\sigma$ decreases from 1 to 0, because $\Delta\sigma$ represents the ability of NA. And the effect of $\Delta\sigma$ on $I(\Delta T)$ has little studied. I/I_0 *vs.* $T_c^{-1}\Delta T^{-1}$ can be simulated as a parameter of
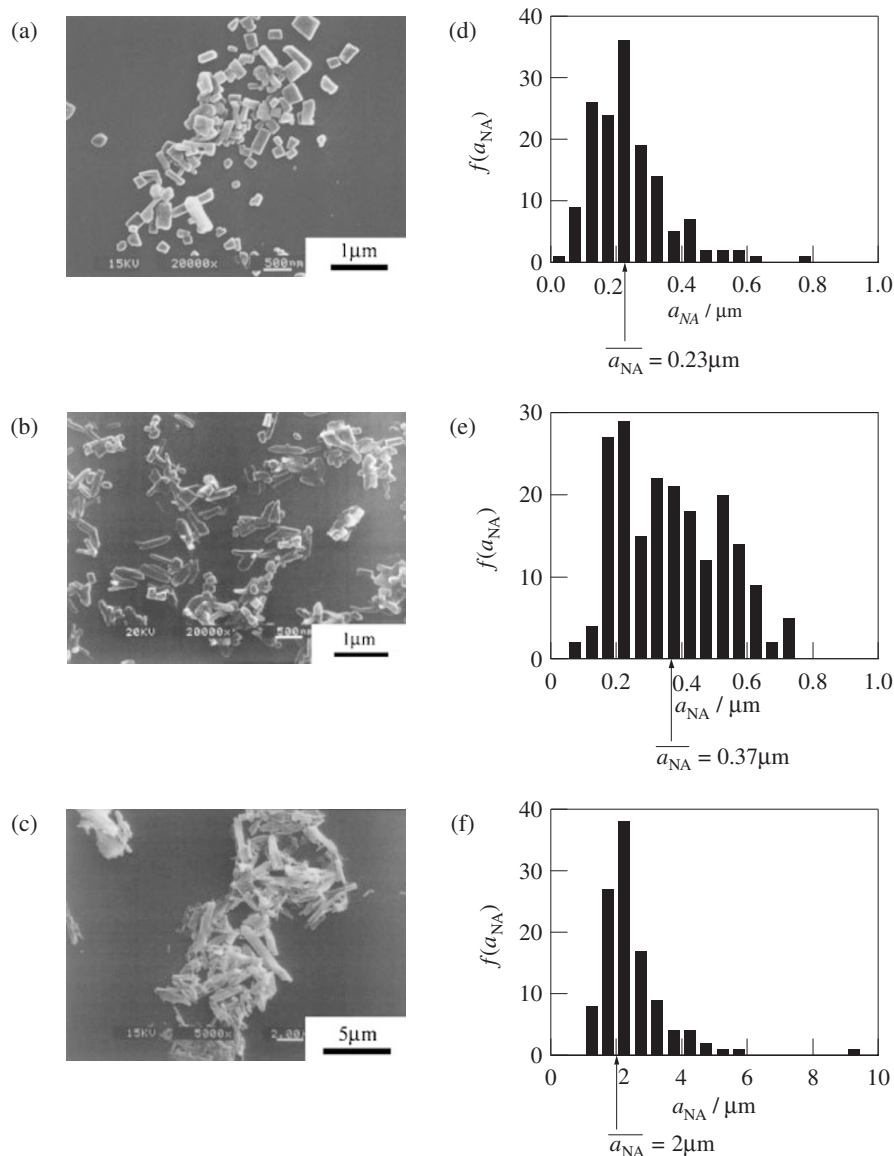
Figure 4. Morphology and $f(a_{NA})$ of NA crystals. Scanning electron micrographs of (a) NA-11, (b) NA-11K and (c) Na-Bz crystals, and $f(a_{NA})$ and $\overline{a_{NA}}$ of (d) NA-11, (e) NA-11K and (f) Na-Bz crystals.
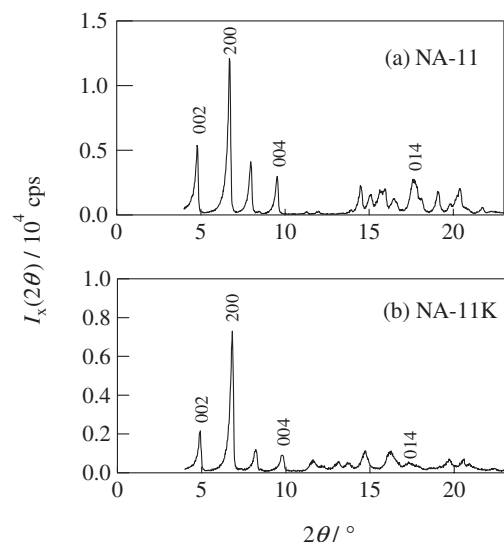
$\Delta\sigma/\sigma$ by using eqs 17, 19 and $\sigma\sigma_e$ from literature. Parameters of iPP are shown in Table I.[9–14] Theoretical curves of I/I_0 against $T_c^{-1}\Delta T^{-1}$ as a parameter of $\Delta\sigma/\sigma$ are shown in Figure 3a. Solid and dotted curves show I_{2D}/I_0 and I_{3D}/I_0, respectively. Nucleus changes from 2D to 3D with decrease of ΔT (*i.e.*, increase of T_c). The conversion from 2D to 3D nucleus is seen at $\Delta T = \Delta T_{2D/3D}$ given by eq 9 which corresponds to $\Delta g = 2\Delta\sigma$. $\Delta T_{2D/3D}$ decreased with decrease of $\Delta\sigma/\sigma$ as shown in Figure 3b. A and B in Figure 3a corresponds to those in Figure 3b. Figure 3c shows the curves of α in eq 20 against $T_c^{-1}\Delta T^{-1}$ as a parameter of $\Delta\sigma/\sigma$. α takes the value which is slightly larger than 1. α increases with increasing $T_c^{-1}\Delta T^{-1}$. With decreasing $\Delta\sigma/\sigma$, α approaches to 1. I/I_0 significantly increase with decrease of $\Delta\sigma/\sigma$. For example, I/I_0 increased by 38 orders of magnitude for $\Delta T = 30\,\mathrm{K}$ and 12 orders of magnitude for $\Delta T = 50\,\mathrm{K}$ with

decreasing $\Delta\sigma/\sigma$ from 1 to 0. In the case of NA where $\Delta\sigma/\sigma < 0.3$, I increases by 10^6 times for $\Delta T = 30\,\mathrm{K}$ and 60 times for $\Delta T = 50\,\mathrm{K}$ with decrease of $\Delta\sigma/\sigma$ from 0.3 to 0. I significantly depends on $\Delta\sigma/\sigma$. Therefore $\Delta\sigma/\sigma$ is essentially important for acceleration of nucleation.

Morphology and Size of NA Crystals

Morphology of NA-11, NA-11K and Na-Bz crystals were observed by means of SEM as shown in Figure 4a, 4b and 4c, respectively. All NA crystals showed rectangular plate shape. As will be shown in Figure 7, NA-11 and NA-11K crystals have the same shape as their large single crystals. The crystals of NAs have a tendency to cleave along the lateral direction. This results in the same shape of grinded crystal as their large single crystal and preservation of epitaxial lattice plane. Size distributions ($f(a_{NA})$) of NA-11, NA-11K and Na-Bz crystals are

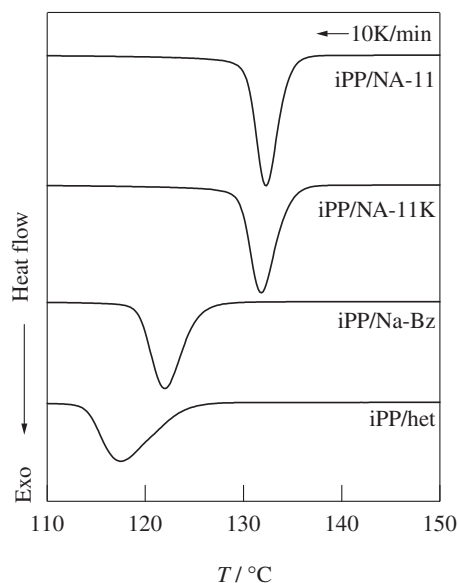**Figure 5.** WAXS diffraction patterns of (a) NA-11 and (b) NA-11K crystals at T_R.

Figure 6. Crystallization behavior of iPP/NAs measured by means of DSC. Cooling rate was 10 K/min. $C_{NA/iPP} = 0.1$ wt %.

shown in Figure 4d, 4e and 4f, respectively. $f(a_{NA})$s of all NA crystals were broad because they were prepared by "top down" method of mechanical grinding as shown in the previous paper.[2] $\overline{a_{NA}}$ of NA-11, NA-11K and Na-Bz crystals were 0.23 μm, 0.37 μm and 2.0 μm, respectively. $\overline{a_{NA}}$ of Na-Bz crystals was much larger than that of NA-11 and NA-11K crystals. As $I \propto \overline{a_{NA}}^{-1}$ was confirmed in the previous study, I of iPP/Na-Bz is expected to be smaller than I of iPP/NA-11 or iPP/NA-11K.

Unit Cell Structure of iPP and NA Crystals

Unit cell structure of iPPs mixed with NAs belongs to α form as shown for iPP/NA-11 in the previous paper.[2] Unit cell structure of NA-11K crystal was determined as the same α form as that of NA-11 crystal,[5] because the WAXS patterns of them were the same in the range of $2\theta = 4 \sim 10°$ as shown in Figure 5. Crystal lattice constant of b of NA-11K (b(NA-11K)) was 0.634 nm. As expected in introduction, b(NA-11K) was larger than b(NA-11). δ' of NA-11K was +2.5%, which is smaller than that of NA-11 (δ'(NA-11) = +6.5%). Thus $\Delta\sigma/\sigma$ of NA-11K is expected to be smaller than that of NA-11.

Effect of NAs on Crystallization Observed by Means of DSC

Crystallization behaviors of iPP/NA-11, iPP/NA-11K, iPP/Na-Bz and iPP observed by means of DSC are shown in Figure 6. C_{NA} was 0.1 wt %. As iPP includes some heterogeneity unintentionally, hereafter we name it iPP/het. Crystallization peak temperature $T_{c,p}$ of iPP/NA-11, iPP/NA-11K, iPP/Na-Bz and iPP/het were 132.3, 131.8, 122.0 and 117.6 °C, respectively. $T_{c,p}$ of iPP/NA-11 and iPP/NA-11K is about 15 °C higher than that of iPP/het. $T_{c,p}$ of iPP/Na-Bz is only 4.4 °C higher than that of iPP/het. This indicates that the ability of Na-Bz as NA is lower than that of NA-11 or NA-11K as will be shown in detail later.
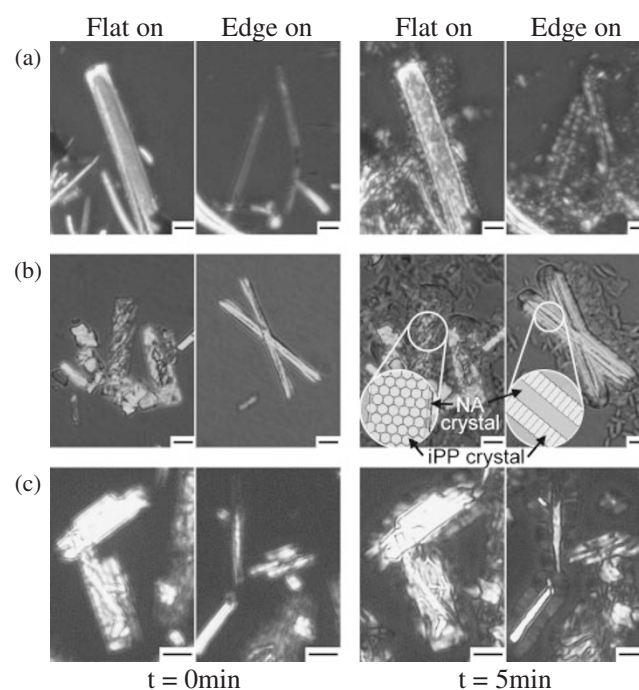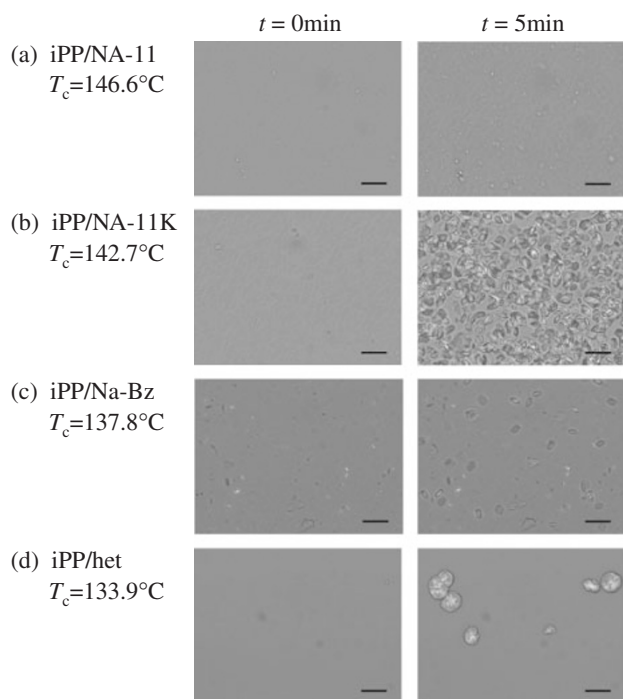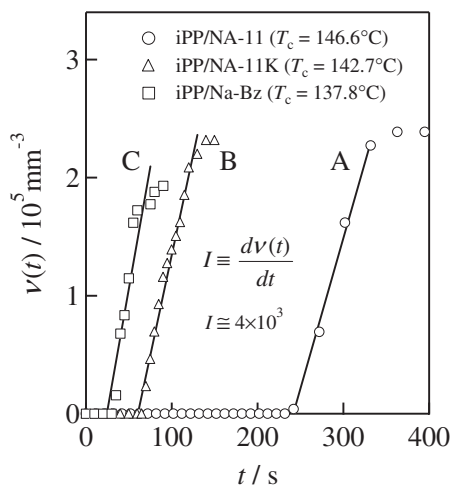

Figure 7. Isothermal crystallization of iPPs mixed with large crystals of (a) NA-11, (b) NA-11K and (c) Na-Bz at $T_c = 138.8$ °C. Scale bar is 10 μm.

Optical Evidence of Epitaxial Growth of iPP on Large Single Crystals of NA

Epitaxial growth of iPP on large single crystals of NA-11, NA-11K and Na-Bz observed at $T_c = 138.8$ °C were shown in Figure 7a, 7b and 7c, respectively. Schematic illustrations of morphology as typical examples are shown in the photograph of Figure 7b (t = 5 min). The iPP lamella crystals grew epitaxially perpendicular to the largest plane of NA crystals.

Figure 8. Isothermal crystallization behavior of (a) iPP/NA-11, (b) iPP/NA-11K, (c) iPP/Na-Bz and (d) iPP/het. $C_{NA/iPP}$ and $\overline{a_{NA}}$ are shown in Table II. Scale bar is 50 μm.

Table II. $\overline{a_{NA}}$ of various NAs and C_{NA}, $\Delta\sigma/\sigma$ and I_0 of iPP/NA-11, iPP/NA-11K, iPP/Na-Bz and iPP/het. $\Delta\sigma/\sigma$ and I_0 were obtained from the fit of eq 19 to the experimental plots

NA	$\overline{a_{NA}}$ (μm)	C_{NA} (wt %)	$\Delta\sigma/\sigma$	I_0 (mm^{-3} s^{-1})
NA-11	0.23	3.9×10^{-2}	0.13	1.3×10^{11}
NA-11K	0.37	1.1×10^{-2}	0.13	2.1×10^{10}
Na-Bz	2.0	3.4×10^{-2}	0.23	1.9×10^{10}
het	—	—	0.23	5.2×10^{7}

Figure 10. Plots of *I*s of iPP/NA-11 ($C_{NA} = 3.9 \times 10^{-2}$ wt %, $a_{NA} = 0.23$ μm), iPP/NA-11K ($C_{NA} = 1.1 \times 10^{-2}$ wt %, $a_{NA} = 0.37$ μm), iPP/Na-Bz ($C_{NA} = 3.4 \times 10^{-2}$ wt %, $a_{NA} = 2$ μm) and iPP/het against $T_c^{-1}\Delta T^{-1}$. Upper axis indicates T_c. Eq 19 was fitted to the plots as parameters of I_0 and $\Delta\sigma/\sigma$. A, B and C corresponds to those in Figure 9.
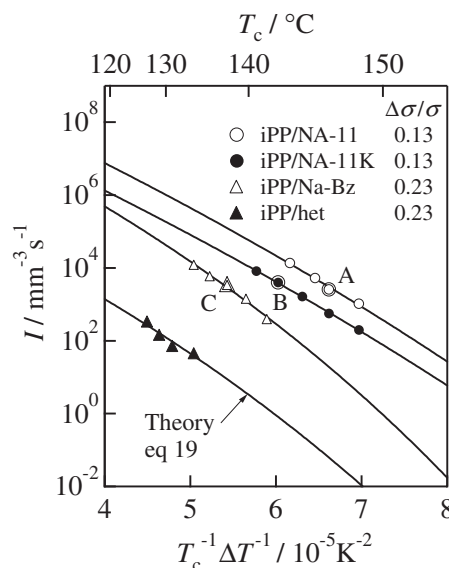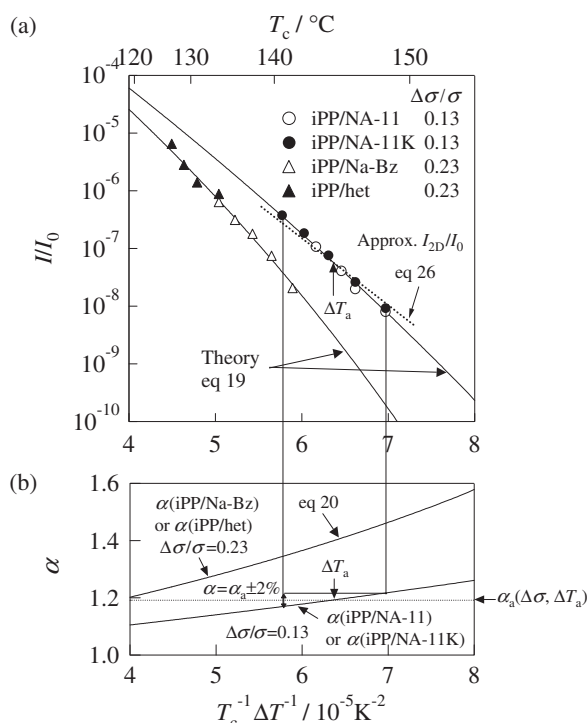

Figure 9. Plots of $\nu(t)$ of iPP/NA-11, iPP/NA-11K and iPP/Na-Bz against t. Nearly the same I was observed at different T_c. A, B and C corresponds to those in Figure 10.

The lamella crystals showed "transcrystal" like morphology. The density of iPP nucleus on the surface of Na-Bz crystal is less than that on the surface of NA-11 and NA-11K crystals. This indicates that efficiency of epitaxy of Na-Bz is lower than that of NA-11 and NA-11K.

Isothermal crystallization behavior of iPP/NA-11, iPP/NA-11K, iPP/Na-Bz and iPP/het are shown in Figure 8a, 8b, 8c and 8d, respectively. T_cs of iPP/NA-11, iPP/NA-11K and iPP/Na-Bz correspond to those in Figure 9, respectively. C_{NA} and $\overline{a_{NA}}$ are shown in Table II. A larger number of iPP crystals

were observed in iPP/NA-11, iPP/NA-11K, and iPP/Na-Bz at higher T_c in comparison with iPP/het. The number of iPP crystals in iPP/NA-11 and iPP/NA-11K is larger than those in iPP/Na-Bz though T_c of iPP/NA-11 and iPP/NA-11K is higher than that of iPP/Na-Bz. Therefore the ability of Na-Bz as NA should be worse than that of NA-11 and NA-11K.

$\Delta G^*(\Delta\sigma)$ Dependence of I

Typical plots of $\nu(t)$ against t are shown in Figure 9. A, B and C indicates iPP/NA-11, iPP/NA-11K and iPP/Na-Bz, respectively. I was obtained from the slope of $\nu(t)$ against t (eq 27). Figure 9 shows that nearly the same Is observed at $T_c = 146.6$, 142.7 and 137.8 °C for iPP/NA-11, iPP/NA-11K and iPP/Na-Bz, respectively.

Log$I$s of iPP/NA-11, iPP/NA-11K, iPP/Na-Bz and iPP/het were plotted against $T_c^{-1}\Delta T^{-1}$ in Figure 10. Upper horizontal axis indicates T_c. $\overline{a_{NA}}$ and C_{NA} are shown in Table II. The plots were fitted by the theoretical curves given by eq 19 as parameters of I_0 and $\Delta\sigma$. For the fitting, the literature value of σ and σ_e in Table I were used.[9,10] All the curves show good fits to the plots. $\Delta\sigma/\sigma$ and I_0 obtained from the fitting are summarized in Table II. $\Delta\sigma/\sigma$ of NA-11K is the same as that

(a)

(b)

Figure 11. (a) Plots of I/I_0s of iPP/NA-11, iPP/NA-11K, iPP/Na-Bz and iPP/het against $T_c^{-1}\Delta T^{-1}$. Upper axis indicates T_c. Solid curves show theoretical I_{2D}/I_0 given by eq 19. Broken line shows approximated I_{2D}/I_0 of iPP/NA-11K given by eq 26. (b) Theoretical plots of α of iPP/NA-11, iPP/NA-11K, iPP/Na-Bz and iPP/het against $T_c^{-1}\Delta T^{-1}$. α_a is the value of α at ΔT_a.

of NA-11 though degree of misfit between NA-11K and iPP crystals is better than that between NA-11 and iPP crystals for an azimuthal orientation (eq 13). Degree of misfit between NA-11K and iPP crystals for the other azimuthal orientation could be larger than that between NA-11 and iPP crystals. $\Delta\sigma/\sigma$ of Na-Bz is much larger than that of NA-11 and the same as that of some heterogeneity in iPP/het.

The plots and curves of I/I_0 against $T_c^{-1}\Delta T^{-1}$ are shown in Figure 11a. As I is divided by I_0, we can discuss ΔG^* dependence of I irrespective of I_0. Upper horizontal axis indicates T_c. I/I_0s of iPP/NA-11 and iPP/NA-11K are the same. I/I_0 of iPP/NA-11 is 2×10^2 times for $\Delta T = 30$ K and 4 times for $\Delta T = 50$ K as large as that of iPP/Na-Bz. Therefore $\Delta\sigma/\sigma$ is significantly important for acceleration of I. I/I_0 increased with decreasing $\Delta\sigma/\sigma$.

The curves of α of iPP/NA-11, iPP/NA-11K, iPP/Na-Bz, and iPP/het against $T_c^{-1}\Delta T^{-1}$ are shown in Figure 11b. As $\Delta\sigma/\sigma$ of iPP/NA-11 and iPP/NA-11K are the same, α of iPP/NA-11 and iPP/NA-11 is the same. α increases with increasing $\Delta\sigma/\sigma$. In the observed range of $T_c^{-1}\Delta T^{-1}$ for iPP/NA-11K, α_a given by eq 24 for $\Delta T_a = 37.5$ K and the difference between α_a and α for $\Delta T_a = 37.5$ K are

$$\alpha_a = 1.19 \quad \text{and} \quad \alpha = \alpha_a \pm 2\%, \tag{28}$$

respectively. Therefore the approximation by eq 24 should be applicable. The dotted line in Figure 11a is the approximated line in eq 26 for iPP/NA-11K ($\alpha_a = 1.19$). The dotted line was

shifted to intersect with the curve of I_{2D}/I_0 of iPP/NA-11K at ΔT_a by changing I_0. The approximated line rather agreed with the fitted line in the narrow range of ΔT. We conclude that the analysis method by the approximation of eq 26 is efficiently to determine $\Delta\sigma$ of polymers in routine work.

CONCLUSIONS

1. Free energy for forming critical nucleus $\Delta G^*(\Delta\sigma)$ is essentially important for acceleration of nucleation where $\Delta\sigma$ is reflected in efficiency of epitaxy. $\Delta G^*(\Delta\sigma)$ dependence of nucleation rate I was evaluated on the basis of nucleation theory. I for the two dimensional nucleus (I_{2D}) is given by

$$\frac{I_{2D}(\Delta\sigma)}{I_0} = \exp\left(-\frac{\Delta G^*_{2D}}{kT_c}\right) = \exp\left\{-\frac{\alpha(\Delta\sigma)\text{B}}{T_c\Delta T}\right\},$$

where I_0 is prefactor, k is Boltzmann constant T_c is crystallization temperature, $\alpha = \Delta g/(\Delta g - \Delta\sigma)$ where Δg is free energy of fusion, B is constant, and ΔT is degree of supercooling. I increased by 38 orders of magnitude for $\Delta T = 30$ K and 12 orders of magnitude for $\Delta T = 50$ K with decrease in $\Delta\sigma/\sigma$ from 1 to 0 where σ is lateral surface free energy of nucleus. In the case $\Delta\sigma/\sigma < 0.3$, I increased by 6 orders of magnitude for $\Delta T = 30$ K and 60 times for $\Delta T = 50$ K with decreasing $\Delta\sigma/\sigma$ from 0.3 to 0. I deeply depends on $\Delta\sigma/\sigma$. Therefore we conclude that $\Delta G^*(\Delta\sigma)$ is essentially important for acceleration of I in heterogeneous nucleation.

2. The evaluation method of $\Delta\sigma$ was established. $\Delta\sigma$ and prefactor I_0 of isotactic polypropylene (iPP) mixed with three nucleating agents (NAs) were obtained from the fit of the above theoretical equation to the experimental plots of I as parameters of $\Delta\sigma$ and I_0. $\Delta\sigma/\sigma$ of sodium 2,2'-methylene-bis-(4,6-di-t-butylphenylene) phosphate (NA-11) and potassium 2,2'-methylene-bis-(4,6-di-t-butylphenylene)phosphate (NA-11K) were 0.13 though degree of misfit for an azimuthal orientation between NA-11K and iPP crystals is better than that between NA-11 and iPP crystals. In the case of sodium benzoate (Na-Bz), $\Delta\sigma/\sigma = 0.23$ was obtained. $\Delta\sigma/\sigma$ of Na-Bz is larger than that of NA-11 or NA-11K. I/I_0 increased with decreasing $\Delta\sigma/\sigma$.

3. I/I_0 of iPP mixed with NA-11 is 2×10^2 times for $\Delta T = 30$ K and 4 times for $\Delta T = 50$ K as large as that of iPP mixed with Na-Bz. Therefore $\Delta\sigma/\sigma$ is significantly important for acceleration of I of polymers by NA.

Appendix: ΔG^* of Lateral Growth

It is well known in CNT that the lateral growth rate V is mainly controlled by the secondary nucleation. V is given by

$$V = V_0 \exp\left\{-\frac{\Delta G^*(2nd)}{\gamma k T_c}\right\} \tag{A·1}$$

where V_0 is a prefactor, $\Delta G^*(2nd)$ is free energy for forming critical nucleus ΔG^* of the secondary nucleus, and $\gamma = 1$ or 3 are single or multi nucleation, respectively.[15] As the secondary

nucleus corresponds to the limit case of the heterogeneous 2D nucleus with $\Delta\sigma = 0$, $\Delta G^*(2nd)$ is given by

$$\Delta G^*(2nd) = \Delta G^*_{2D}(\Delta\sigma = 0)$$
$$= \frac{4(\sigma\sigma_e)}{\Delta g} = \left\{\frac{4(\sigma\sigma_e)T^0_m}{\Delta h}\right\}\frac{1}{\Delta T}. \quad (A\cdot2)$$

Insertion of eq A·2 into eq A·1 gives

$$\frac{V}{V_0} = \exp\left\{-\frac{\Delta G^*(2nd)}{\gamma kT_c}\right\} = \exp\left(-\frac{B}{\gamma T_c\Delta T}\right) \quad (A\cdot3)$$

where $B = \dfrac{4(\sigma\sigma_e)T^0_m}{k\Delta h}$. $\quad (A\cdot4)$

$(\sigma\sigma_e)$ can be obtained from the slope of the plots of V against $T_c^{-1}\Delta T^{-1}$, *i.e.*, $-B/\gamma$.

REFERENCES

1. K. Okada, K. Watanabe, T. Urushihara, A. Toda, and M. Hikosaka, *Polymer*, **48**, 401 (2007).
2. T. Urushihara, K. Okada, K. Watanabe, A. Toda, E. Tobita, N. Kawamoto, and M. Hikosaka, *Polym. J.*, **39**, 55 (2007).
3. R. Becker and W. Döring, *Ann. Phys.*, **24**, 719 (1935).
4. D. Turnbull and J. C. Fisher, *J. Chem. Phys.*, **17**, 71 (1949).
5. F. P. Price, in "Nucleation," A. C. Zettlemoyer, Ed., Marcel Dekker, New York, 1969, chap. 8, p 405.
6. Y. Takeda, in "Epitakisharu Seityono Mekanizumu (Mechanism of epitaxial growth)," K. Nakajima, ed., Kyoritsu Shuppan, Tokyo, 2002, chap. 5, p180.
7. S. Yoshimoto, T. Ueda, K. Yamanaka, A. Kawaguchi, E. Tobita, and T. Haruna, *Polymer*, **42**, 9627 (2001).
8. M. Hikosaka and T. Seto, *Polym. J.*, **5**, 111 (1973).
9. E. J. Clark and J. D. Hoffmann, *Macromolecules*, **17**, 878 (1984).
10. K. Yamada, M. Hikosaka, A. Toda, S. Yamazaki, and K. Tagashira, *J. Macromol. Sci. Part B, Phys.*, **42**, 733 (2003).
11. J. Brandrup, E. H. Immergut, D. R. Bloch, and E. A. Grulke, in "Polymer Handbook," 4th ed., John Wiley & Sons, New York, 2003, V/23.
12. J. J. Janimak, S. Z. D. Cheng, and P. A. Giusti, *Macromolecules*, **24**, 2253 (1991).
13. K. Yamada, M. Hikosaka, A. Toda, S. Yamazaki, and K. Tagashira, *Macromolecles*, **36**, 4790 (2003).
14. K. Yamada, M. Hikosaka, A. Toda, S. Yamazaki, and K. Tagashira, *Macromolecles*, **36**, 4802 (2003).
15. A. Ohkawa, in "Kessho-Seicho (Crystal Growth)," Shokabo Publishing, Tokyo, 1977, chap. 1, p 23.